

On gravito-magnetic time delay by extended lenses

M. Sereno^{1,2,3?}

¹Dipartimento di Scienze Fisiche, Università degli Studi di Napoli "Federico II", Via Cintia, Monte S. Angelo, 80126 Napoli, Italia

²Istituto Nazionale di Astrofisica - Osservatorio Astronomico di Capodimonte, Salita M. S. Angelo, 16, 80131 Napoli, Italia

³Istituto Nazionale di Fisica Nucleare, Sez. Napoli, Via Cintia, Monte S. Angelo, 80126 Napoli, Italia

13 September, 2004

ABSTRACT

Gravitational lensing by rotating extended detectors is discussed. Due to spin, corrections on image positions, caustics and critical curves can be significant. In order to obtain realistic quantitative estimates, the lens is modeled as a singular isothermal sphere. Gravitomagnetic time delays of ~ 0.2 days between different images of background sources can occur.

Key words: astrometry { gravitation { gravitational lensing { relativity

1 INTRODUCTION

Mass-energy currents relative to other masses generate space-time curvature. This phenomenon, known as intrinsic gravitomagnetism, is a new feature of general theory of relativity and other conceivable post-Newtonian theories of gravity (see Ciufolini & Wheeler 1995, and references therein). The gravitomagnetic field has not been yet detected with high accuracy. Some results have been reported from laser-ranged satellites, when the Lense-Thirring precession, due to the Earth spin, was measured by studying the orbital perturbations of LAGEOS and LAGEOS II satellites (Ciufolini & Pavlis 1998, 2004). According to a preliminary analysis, the predictions of the general theory of relativity have been found to agree with the experimental values within the 10 per cent accuracy (Ciufolini & Pavlis 2004). The NASA's Gravity Probe B satellite should improve this measurement to an accuracy of 1 per cent. Intrinsic gravitomagnetism might play a relevant role also in the dynamics of the accretion disk of a supermassive black hole or in the alignment of jets in active galactic nuclei and quasars (Ciufolini & Wheeler 1995).

Whereas the tests just mentioned limit to the gravitational field outside a spinning body, the general theory of relativity predicts peculiar phenomena also inside a rotating shell (see Weinberg 1972, for example). Gravitational lensing can represent a tool to fully test the effects of the gravitomagnetic field (see Sereno (2003a) and reference therein). In this paper, we are interested in the gravitomagnetic time delay induced in different images of the same source due to gravitational lensing. Whereas here we are mainly faced with intrinsic gravitomagnetism, i.e. with spinning detectors, a translational motion of the lens can also induce interesting phenomena, which in the framework of general relativity are

strictly connected to the Lorentz transformation properties of the gravitational field. The effect of the detector's velocity has been recently observed in the Jovian deflection experiment conducted at VLBI, which measured the time delay of light from a background quasar (Fomalont & Kopeikin 2003). Although a controversy has emerged over the theoretical interpretation of this measurement (Kopeikin 2004), there is agreement about the role of the detector's motion.

Gravitational time delay by spinning detectors has been addressed by several authors with very different approaches. Dymnikova (1986) discussed the additional time delay due to rotation by integrating the light geodesics of the Kerr metric. Using the Lense-Thirring metric, Gilstein (1999) considered the time delay for light rays passing outside a spinning star. Kopeikin and collaborators (Kopeikin 1997; Kopeikin & Schäfer 1999; Kopeikin & Mashhoon 2002) analysed the gravitomagnetic effects in the propagation of light in the field of self-gravitating spinning bodies. The gravitational time delay due to rotating masses was further discussed in Ciufolini et al. (2003); Ciufolini & Ricci (2003), where the cases of light rays crossing a slowly rotating shell or propagating in the field of a distant source were analyzed in the linear approximation of general theory of relativity. Effects of an intrinsic gravitomagnetic field were further studied in the usual framework of gravitational lensing theory (Sereno 2002, 2003b,a; Sereno & Cardone 2002), i.e. i) weak field and slow motion approximation for the lens and ii) thin lens hypothesis (Schneider et al. 1992; Petters et al. 2001). Expressions for bending and time delay of electromagnetic waves were found for stationary spinning detectors with general mass distributions (Sereno 2002).

The paper is as follows. In Section 2, basics of gravitational lensing by a stationary extended detector are reviewed. In Section 3, we introduce our reference model for the lens, i.e. a spinning singular isothermal sphere. Relevant lensing quantities for such a deflecting system are de-

? E-mail: mauro.sereno@na.infn.it

rived in Section 4. In Section 5, the lens equation is solved. A quantitative discussion of the gravito-magnetic time delay is in Section 6, where we also investigate the effect on the determination of the Hubble constant. Section 7 is devoted to some final considerations. Unless otherwise stated, throughout this paper we consider a flat cosmological model of universe with cosmological constant and a pressureless cosmological density parameter $\Omega_M = 0.3$ a Hubble constant $H_0 = 72 \text{ km s}^{-1} \text{ Mpc}^{-1}$.

2 GRAVITO-MAGNETIC DEFLECTION POTENTIAL

Gravitational lensing theory can be easily developed in the gravitational field of a rotating stationary source when the linear approximation of general relativity holds (Sereno 2002). The time delay of a kinematically possible ray, with impact parameter b in the lens plane, relative to the unlensed one is, for a single lens plane, (Sereno 2002)

$$\tau = \frac{(1+z_d)}{c} \frac{1}{2} \frac{D_d D_s}{D_{ds}} \frac{1}{D_d} \frac{1}{D_s} \hat{\alpha}(\theta); \quad (1)$$

where $\hat{\alpha}$ is the deflection potential; D_s , D_d and D_{ds} are the angular diameter distances between observer and source, observer and lens and lens and source, respectively; z_d is the lens redshift; θ is the bidimensional vector position of the source in the source plane. We have neglected a constant term in equation (1), since it has no physical significance (Schneider et al. 1992).

The deflection potential can be expressed as the sum of two terms

$$\hat{\alpha} = \hat{\alpha}_0 + \hat{\alpha}_{\text{GRM}}; \quad (2)$$

the main contribution is

$$\hat{\alpha}_0(\theta) = \frac{4G}{c^2} \int_{<2}^Z d^2 \theta' \int_0^{\infty} \ln \frac{|\theta - \theta'|}{r_0} \rho(\theta', l) dl; \quad (3)$$

where r_0 is a length scale in the lens plane and ρ is the projected surface mass density of the deflector,

$$\rho(\theta) = \int_0^{\infty} \rho(\theta, l) dl; \quad (4)$$

the gravito-magnetic correction to the deflection potential, up to the order $v=c$, can be expressed as (Sereno 2002)

$$\hat{\alpha}_{\text{GRM}} = \frac{8G}{c^4} \int_{<2}^Z d^2 \theta' \int_0^{\infty} \ln \frac{|\theta - \theta'|}{r_0} \langle v_{\parallel} \rangle(\theta', l) dl; \quad (5)$$

where $\langle v_{\parallel} \rangle$ is the weighted average, along the line of sight e_{in} , of the component of the velocity v along e_{in} ,

$$\langle v_{\parallel} \rangle(\theta) = \frac{\int_0^{\infty} (v(\theta, l) \cdot e_{\text{in}}) dl}{\rho(\theta)}; \quad (6)$$

In the thin lens approximation, the only components of the velocities parallel to the line of sight enter the equations of gravitational lensing. We remind that the time delay function is not an observable, but the time delay between two actual rays can be measured. Similar results, based on a multipolar description of the gravitational field of a stationary lens, can be found in Kopeikin (1997).

3 SINGULAR ISOTHERMAL SPHERE

Isothermal spheres are widely used in astrophysics to understand many properties of systems on very different scales, from galaxy halos to clusters of galaxies (Mo et al. 1998; Schneider et al. 1992). In particular, on the scale relevant to interpreting time delays, isothermal models are favoured by data on early-type galaxies (Kochanek & Schechter 2004). The density profile of a singular isothermal sphere (SIS) is

$$\rho(r) = \frac{v^2}{2G} \frac{1}{r^2}; \quad (7)$$

where v is the velocity dispersion. The corresponding projected mass density is

$$\Sigma(r) = \frac{v^2}{2G} \frac{1}{r}; \quad (8)$$

Since the total mass is divergent, we introduce a cut-off radius R_{SIS} . The cut-off radius of the halo must be much larger than the relevant length scale which characterizes the phenomenon, in order to not significantly affect the lensing behavior. The total mass of a truncated SIS is

$$M_{\text{SIS}} = \frac{2}{G} v^2 R_{\text{SIS}}; \quad (9)$$

A limiting radius can be defined as r_n , the radius within which the mean mass density is n times the critical density of the universe at the redshift of the galaxy, z_d . For a SIS, it is

$$r_n = \frac{2}{nH(z_d)} v; \quad (10)$$

where H is the time dependent Hubble parameter.

The total angular momentum of a halo, J , can be expressed in terms of a dimensionless spin parameter λ , which represents the ratio between the actual angular velocity of the system and the hypothetical angular velocity that is needed to support the system (Padmabhan 2002),

$$J = \frac{GM^2}{E} \lambda; \quad (11)$$

where M and E are the total mass and the total energy of the halo, respectively. In the hypothesis of initial angular momentum acquired from tidal torquing, typical values of λ can be obtained from the relation between energy and virial radius and the details of spherical top-hat model (Padmabhan 2002). As it was derived from numerical simulations, the distribution of λ is nearly independent of the mass and the power spectrum. It can be approximated by a log-normal distribution (Vitvitska et al. 2002)

$$p(\lambda) d\lambda = \frac{1}{\sigma} \exp\left[-\frac{(\ln \lambda - \mu)^2}{2\sigma^2}\right] \frac{d\lambda}{\lambda}; \quad (12)$$

with $\mu = 0.05$ and $\sigma = 0.5$. The distribution peaks around $\lambda = 0.04$ and has a width of ≈ 0.05 .

From the virial theorem, the total energy is easily obtained (Mo et al. 1998)

$$E_{\text{SIS}} = -\frac{1}{2} M_{\text{SIS}} v^2; \quad (13)$$

Finally, the total angular momentum of a truncated SIS can be written as

$$J_{\text{SIS}} = \frac{4}{3} \frac{v^3 R_{\text{SIS}}^2}{G}; \quad (14)$$

In general, the angular velocity of a halo is not constant and a differential rotation should be considered (Capozziello et al. 2003). However, assuming a detailed rotation pattern does not affect significantly the results. In what follows, we will consider the case of constant angular velocity.

4 LENSING BY A ROTATING SIS

Let us consider gravitational lensing by a SIS in rigid rotation, i.e. with a constant angular velocity ω , about an arbitrary axis passing through its center. The deflection angle can be written as (Serenio & Cardone 2002)

$$\hat{\alpha}_1^{SIS}(\xi; \theta) = 4 \frac{v}{c} \frac{2^n}{h} \cos \theta + \frac{\omega_1}{c} \frac{\sin 2\theta}{3} \frac{1}{R_{SIS}} \frac{1}{\xi} \frac{1}{\theta} ; \quad (15)$$

$$\hat{\alpha}_2^{SIS}(\xi; \theta) = 4 \frac{v}{c} \frac{2^n}{h} \sin \theta + \frac{\omega_2}{c} \frac{\sin 2\theta}{3} \frac{1}{R_{SIS}} \frac{1}{\xi} \frac{1}{\theta} + \frac{\omega_1}{c} \frac{\cos 2\theta}{3} \frac{1}{1 + R_{SIS}} ; \quad (16)$$

where $(\xi; \theta)$ are polar coordinates in the lens plane and ω_1 and ω_2 are the components of ω along the x_1 - and the x_2 -axis, respectively. The parameter ω has to be interpreted as an effective angular velocity $\omega = J_{SIS} = I_{SIS} \omega$ where I_{SIS} is the central moment of inertia of a truncated SIS, $I_{SIS} = 2 = 9M_{SIS} R_{SIS}^2$. In terms of the spin parameter,

$$\omega = 9 \frac{v}{R_{SIS}} ; \quad (17)$$

Equations (15) and (16) correct the result in equation (9) in Capozziello & Re (2001), which was obtained under the same assumptions but was affected by an error in the computation of the integrals. For a SIS, there are two main contributions to the gravito-magnetic correction to the deflection angle (Serenio & Cardone 2002): the first contribution comes from the projected moment of inertia inside the radius r ; the second contribution is due to the mass outside r and can become significant in the case of a very extended lens, i.e. for a very large cut-off radius.

Let us consider a sphere rotating about the x_2 -axis, $\omega_1 = 0; \omega_2 = \omega$. In order to change to dimensionless variables, we introduce a length scale,

$$r_0 = R_E = 4 \frac{v}{c} \frac{2^n}{c} \frac{D_d D_{ds}}{D_s} ; \quad (18)$$

The dimensionless position vector in the lens plane is $\mathbf{x} = \mathbf{x}_0$. The dimensionless deflection potential,

$$\frac{D_d D_{ds}}{D_s^2} \hat{\alpha} \quad (19)$$

can be written as

$$\hat{\alpha}^{SIS}(\mathbf{x}_1; \mathbf{x}_2) = \mathbf{x} \left(\frac{3}{2} r - \mathbf{x} \right) L \mathbf{x}_1 ; \quad (20)$$

where $\mathbf{x} = \mathbf{x}_j$ and $L = (2=3) (\omega R_E = c)$ is an estimate of the rotational velocity and r is the cut-off radius in units of R_E . When $L > 0$, the angular momentum of the lens is positively oriented along \hat{x}_2 . The dimensionless Fermat potential is defined as,

$$\phi(\mathbf{x}; \mathbf{y}) = \frac{1}{2} (\mathbf{x} - \mathbf{y})^2 - \hat{\alpha}(\mathbf{x}); \quad (21)$$

where $\mathbf{y} = \frac{D_s}{D_d} \mathbf{y}_0$.

The scaled deflection angle is related to the dimensionless gravitational potential

$$\hat{\alpha}(\mathbf{x}) = r - \phi(\mathbf{x}); \quad (22)$$

We get

$$\hat{\alpha}_1^{SIS}(\mathbf{x}_1; \mathbf{x}_2) = \frac{x_1}{x} + L \frac{2x_1^2 + x_2^2}{x} \frac{3}{2} r ; \quad (23)$$

$$\hat{\alpha}_2^{SIS}(\mathbf{x}_1; \mathbf{x}_2) = \frac{x_2}{x} + L \frac{x_1 x_2}{x} ; \quad (24)$$

The determinant of the Jacobian matrix reads

$$A_{SIS}(\mathbf{x}_1; \mathbf{x}_2) = 1 - \frac{1}{x} \frac{L x_1}{x} \frac{3}{x} \frac{2}{x} ; \quad (25)$$

The convergence $k = \sigma_{cr}$ is the projected density in units of the critical surface density,

$$\sigma_{cr} = \frac{c^2}{4 G D_d D_{ds}} ; \quad (26)$$

It is

$$k_{SIS} = \frac{1 + 3L x_1}{2x} ; \quad (27)$$

k_{SIS} is positive when $x_1 > 1=3L$. Since we have introduced a cut-off radius, this condition holds for $x_1 < r$. The condition $L r < 1=3$ warrants that $k_{SIS} > 0$ for all points in the lens plane.

5 THE LENS EQUATION

In general, the inversion of the lens equation is a mathematical demanding problem. However, since the gravito-magnetic effect in the weak field limit is a higher-order correction, a rotating system can be studied in some details using a perturbative approach (Serenio 2003a). The lens equation can be expressed in a dimensionless form as

$$\mathbf{y} = \mathbf{x} - \hat{\alpha}(\mathbf{x}); \quad (28)$$

The unperturbed images are solutions of the lens equation for $L = 0$. When $y = |y_j| < 1$, a static SIS lens produces two images, collinear with the source position and the lens centre, at radii $x = y + 1$ and $x = y - 1$. When $y > 1$, only one image forms, at $x = y + 1$.

Under the condition $L \ll 1$, we can obtain approximate solutions to the first-order in L , given by

$$\mathbf{x} = \mathbf{x}_{(0)} + L \mathbf{x}_{(1)} ; \quad (29)$$

where $\mathbf{x}_{(0)}$ and $\mathbf{x}_{(1)}$ denote the zeroth-order solution (i.e. the solution of the lens equation for $L = 0$), and the correction to the first-order, respectively. By substituting equation (29) in the vectorial lens equation, equation (28), we obtain the first-order perturbations,

$$\mathbf{x}_{(1)1} = \mathbf{x}_{(0)}^2 + \frac{3}{2} r - 2\mathbf{x}_{(0)} + \mathbf{x}_{(0)}^2 \frac{\mathbf{x}_{(0)1} \mathbf{x}_{(0)}^2}{\mathbf{x}_{(0)}^2 (\mathbf{x}_{(0)} - 1)} ; \quad (30)$$

$$\mathbf{x}_{(1)2} = \frac{3}{2} r - 2\mathbf{x}_{(0)} + \mathbf{x}_{(0)}^2 \frac{\mathbf{x}_{(0)1} \mathbf{x}_{(0)2}}{\mathbf{x}_{(0)}^2 (\mathbf{x}_{(0)} - 1)} ; \quad (31)$$

For a source on the y_1 -axis ($y_2 = 0$), equations (30) and (31) reduce to

$$\mathbf{x}_{(1)1} = \frac{3}{2} r + 2\mathbf{x}_{(0)1} ; \quad (32)$$

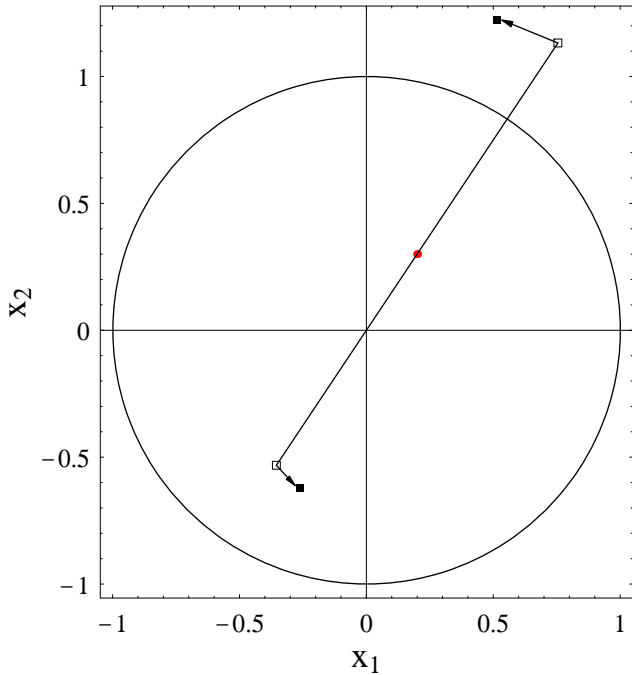


Figure 1. Image positions (square boxes) and critical line (full line) for a rotating SIS lens. The source is the grey circle. The centre of the coordinate axes, the source and the two unperturbed images (empty boxes) lie on a straight line. Two images (filled boxes) are counter-clockwise rotated, about the line of sight through the centre, with respect to this line. It is $L = 10^{-3}$ and $r = 50$.

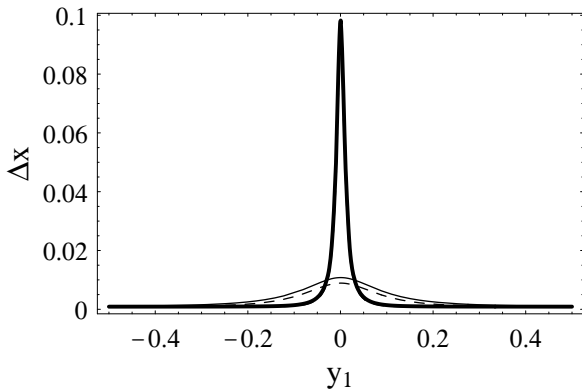


Figure 2. The shift in the image positions (in units of arcsec) due to the gravito-magnetic field for source moving parallelly to the y_1 -axis. Thick and thin lines are for $y_2 = 0.01$ and 0.1 , respectively. Full and dashed lines refer to the two images. It is $L = 4 \cdot 10^5$ and $r = 15$.

$$x_{(1)2} = 0; \tag{33}$$

When $L > 0$, photons with an impact parameter $x_1 < 0$ ($x_1 > 0$) go around the lens in the same (opposite) sense of the detector. Due to the contribution to the deflection angle from the mass outside the impact parameter, photons which impact the lens plane on the x_1 -axis at $x_1 > 0$ move closer to the centre. This feature, which is peculiar of light rays propagating inside a halo, is opposite to the case of propagation

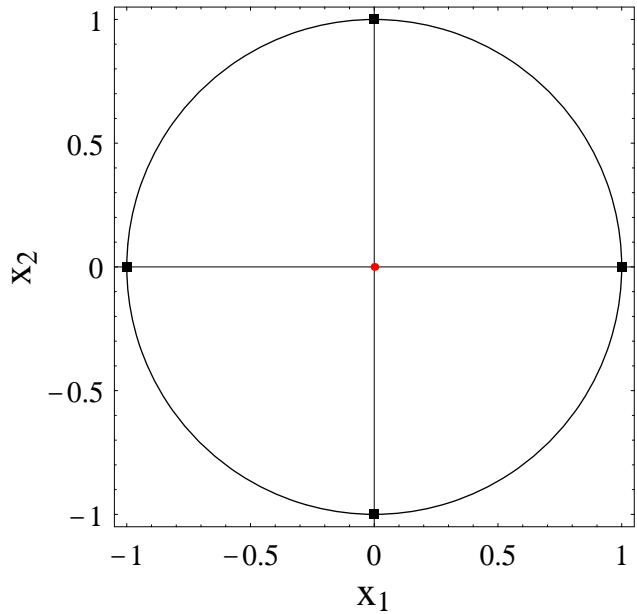


Figure 3. A source (the grey circle) inside the central caustic of a rotating SIS is multiple imaged in a cross shaped pattern; the four filled boxes locate the four images. The critical line is also plotted. It is $r = 15$ and $L = 3.5 \cdot 10^5$.

outside a spinning sphere (Sereno 2003a), when photons in the equatorial plane moving in the same (opposite) sense of rotation of a detector form closer (farther) images with respect to the non-rotating case. In fact, in the last case, there is no mass outside the photon path. If we do not limit to the equatorial plane, for $L > 0$, the images are rotated counter-clockwise around the line of sight with respect to the static case, see Figure 1.

Let us consider the gravito-magnetic correction to the deflection angle for a typical galaxy lens at $z_d = 0.3$ with $v = 250 \text{ km s}^{-1}$, $R_{\text{SIS}} \leq 100 \text{ Kpc}$ and $\theta = 0.1$, and a background quasar at $z_s = 2.0$. Such a configuration corresponds to $L = (2-4) \cdot 10^5$ and $r = 15$. For some particular source positions, the shift in the image positions in the lens plane with respect to the static case can be as large as $0.1''$. In Figure 2, we plot the shift in the image positions for a source moving along the y_1 -axis, i.e. for $y_2 = \text{const}$: The maximum variation occurs when the source nearly crosses the projected rotation axis.

The critical curve is slightly distorted. The solution of $\det A(x_1; x_2) = 0$, with respect to x_2 , is

$$x_2(x_1) = \frac{p}{1 - x_1^2} + \frac{x_1}{1 - x_1^2} L; \tag{34}$$

The area of the critical curve slightly grows and its centre shifts of L along the x_1 -axis. The critical curve intersects the x_1 -axis in $x_1 = L - 1$. The changes in the width and in the height of the critical curve are of order $O(L^2)$.

The four extremal points of the critical curve can be mapped onto the source plane through the lens equation to locate the cusps of the caustic. We find a diamond-shaped caustic with four cusps, centred in $(y_1; y_2) = (L(\frac{1}{2}r - 1); 0)$. The axes, of semi-width L^2 , are parallel

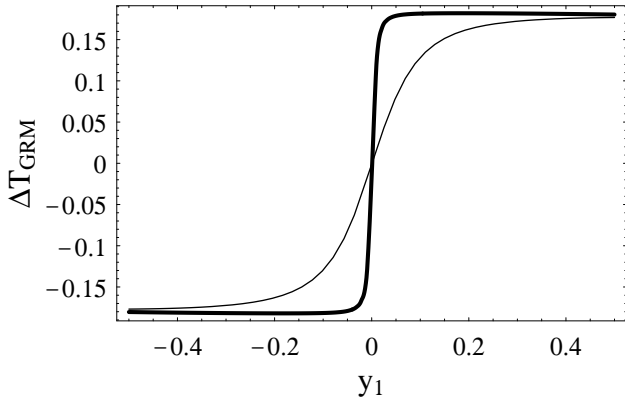


Figure 4. The gravito-magnetic time delay (in units of days) for a source moving parallelly to the y_1 -axis. Thick and thin lines are for $y_2 = 0.01$ and 0.1 , respectively. It is $L = 4 \cdot 10^{-5}$ and $r = 15$.

to the coordinate axes. The orientation and the position on the caustic depends on both the strength and orientation of the angular momentum and on the radius of the lens. When the source is inside the caustic, two additional images form. Since the axial symmetry is broken by the gravito-magnetic field, the Einstein ring is no more produced. A source, which is inside the central caustic, is imaged in a cross pattern, see Fig. 3.

6 TIME DELAY

As we have seen in Section 2, the time delay for a spinning SIS is made of three main contributions: the geometrical time delay, t_{geom} , the unperturbed gravitational time delay by a static SIS, t_0 , and, finally, the gravito-magnetic time delay, t_{GRM} ,

$$t' = t_{\text{geom}} + t_0 + t_{\text{GRM}} \quad (35)$$

The main contribution to the gravitational time delay of a light ray with respect to the unperturbed path can be rewritten as

$$ct_0 = 4(1 + z_d)D_d \frac{v}{c}^2; \quad (36)$$

where θ is the modulus of the angular position in the lens plane, $\theta = \theta_d = D_d$. The gravito-magnetic time delay is

$$ct_{\text{GRM}} \approx 24 \frac{v}{c}^3 (1 + z_d)D_d \frac{3}{2} \frac{1}{\theta_{\text{SIS}}} \quad (37)$$

$$\approx 36 \frac{v}{c}^3 (1 + z_d)D_d \theta_1 \quad (38)$$

where θ_1 is the angular distance of an image from the projected rotation axis and $\theta_{\text{SIS}} = R_{\text{SIS}}/D_d$. To obtain equation (38), we have used the relation $x = r$. An approximate relation holds between t_0 and the gravito-magnetic time delay,

$$t_{\text{GRM}} \approx 9 \cos^2 \theta \frac{v}{c} t_0 \quad (39)$$

Since $L \ll 1$, the angular separation between the two images is nearly

$$\theta \approx 8 \frac{v}{c} \frac{D_{\text{ds}}}{D_s}; \quad (40)$$

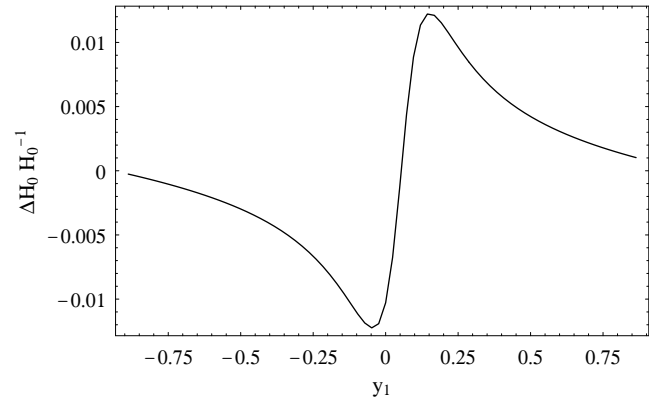


Figure 5. Relative error in the estimate of the Hubble constant, due to neglecting the gravito-magnetic field, for a source moving with fixed $y_2 = 0.1$. It is $L = 2.5 \cdot 10^{-3}$ and $r = 15$.

and the gravito-magnetic induced retardation between the two images, $T_{\text{GRM}} = t_{\text{GRM}}(x_a) - t_{\text{GRM}}(x_b)$, can be approximated as

$$c T_{\text{GRM}} \approx 288 \cos^2 \theta \frac{D_{\text{ds}} D_d}{D_s} \frac{v}{c}^5; \quad (41)$$

Since the two images are nearly collinear with the lens centre, the gravito-magnetic time delay is nearly independent of the cut-off radius.

For a typical lensing galaxy at $z_d = 0.5$ with $v = 250 \text{ km s}^{-1}$, and a background source at $z_s = 2.0$, the gravito-magnetic time delay is $0.1 - 0.2$ days for $0.05 - 0.1$. In Fig. 4, the time delay between the images is plotted as a function of the source position for a source moving perpendicularly to the projected rotation axis. The distance of the source from the y_1 -axis determines the width of the transition between the extremal values.

6.1 The Hubble constant

Any gravitational lensing system can be used to determine the Hubble constant (Refsdal 1964). Neglecting the gravito-magnetic correction can induce an error in the estimate of the Hubble constant. In general, it is

$$H_0 t = F(v; z_d; z_s; \theta); \quad (42)$$

where the dimensionless function F depends on the lens parameters and on the cosmological density parameters, but the latter dependence is not very strong. A lens model which reproduces the positions and magnifications of the images provides an estimate of the scaled time delay $H_0 t$ between the images. Therefore, a measurement of t will yield the Hubble constant. Let us consider a rotating galaxy, described by a SIS with known dispersion velocity and redshift, which forms multiple images of a background quasar at redshift z_s . An observer can measure the time delay between the two images, T_{obs} , and their positions, x_a and x_b . The unknown source position y can be obtained by inverting the lens equation. In terms of the dimensionless Fermat potential ψ , the measured Hubble constant turns out to be

$$H_0 = \frac{1}{T_{\text{obs}}} F(z_d; z_s; v; y)(x_a; y) - (x_b; y); \quad (43)$$

where

$$F(z_d; z_s; v) = (1 + z_d)^{-4} \frac{v}{c} \frac{r_d r_{ds}}{r_s} \quad (44)$$

and r is the angular diameter distance in units of c/H_0 .

If, we assume a static lens model to model the data, the estimated Hubble constant is

$$H_0^{ST} = \frac{1}{T_{obs}} F(z_d; z_s; v) 2y^{ST} \quad (45)$$

where the "not correct" estimated position of the source is

$$y^{ST} = \frac{1}{2} \sum_{a,b} x_i \frac{x_i}{k_i} \quad (46)$$

The relative error in the determination of the Hubble constant is

$$\frac{H_0}{H_0} = \frac{2y^{ST} \sum_j (x_{aj} y_j) (x_{bj} y_j)}{\sum_j (x_{aj} y_j) (x_{bj} y_j)} \quad (47)$$

For a source at fixed y_2 , the maximum error is $1 = 2 \sum_j y_j$; see Fig. 5. Since usually $L < 10^4$, the induced relative error is really negligible.

7 DISCUSSION

Since the physics of gravitational lensing is well understood, the gravito-magnetic time delay may provide a new observable for the determination of the total mass and angular momentum of the lensing body (Ciufolini & Ricci 2003). Although a detailed model may be required to reproduce the overall mass distribution in the lens, interpretation of time delay is based on a limited number of parameters. Provided the cluster where the deflector lies can be described by a simple expansion, the only parameters needed to model the time delay are those needed to vary the average surface density of the lens near the images and to change the ratio between the quadrupole moment of the lens and the environment (Kochanek & Schechter 2004). Furthermore, the presence of an observed Einstein ring can provide strong independent constraints on the mass distribution.

We have developed our treatment of the gravito-magnetic time delay by modeling the lens as a SIS. Isothermal models are supported by both theoretical prejudices and estimates from observations of early-type galaxies so that SIS turns out to be a surprisingly realistic starting point for modeling lens potentials. Gravitomagnetic time delays of

0.1-0.2 days can be produced in typical lensing systems. A broad range of methods for reliably determining time delays from typical data and a deep understanding of the systematic problems has been developed in last years. Time delay estimates are more and more accurate and an accuracy of 0.2 days has been already obtained in the case of B0218+357 (Biggs et al. 1999), so that the detection of the gravito-magnetic time delay will be soon within astronomers' reach. Observations with radio interferometers or HST can measure the relative positions of the images and lenses to accuracies $< 0:005^{\text{mas}}$. Shifts in the image positions due to a gravito-magnetic field are usually well above this limit.

Our results are nearly unaffected by the presence of low-mass satellites and stars. These substructures do not have any impact on time delays and can only produce random perturbations of approximately $0:001^{\text{mas}}$ in image posi-

tions (Kochanek & Schechter 2004), quite below the gravito-magnetic effect. Deviations from circular symmetry due to either the ellipticity of the deflector or the local tidal gravity field from nearby objects should be considered too. However, for a singular isothermal model with arbitrary structure, the time delays turn out to be independent of the angular structure (Kochanek & Schechter 2004). Other higher-order effects, such as the delay due to the quadrupole moment of the deflector, should be considered in addition to the gravito-magnetic time delay. Unlike other effects, a gravito-magnetic field can break the circular symmetry of the lens, inducing characteristic features in lensing events (Sereno 2003b). At least in principle and for some configurations of the images, a suitable combination of the observable quantities can be used to remove additional effects, due to a quadrupole moment, from observational data (Ciufolini & Ricci 2002; Ciufolini et al. 2003). Furthermore, when the lensed images lie on opposite sides of the lens galaxy, the time delay becomes nearly insensitive to the quadrupole structure of the deflector (Kochanek & Schechter 2004).

Measurements of gravito-magnetic time delays could offer an interesting perspective to address the "angular momentum problem". Cold dark matter models of universe with a substantial cosmological constant appear to fit large scale structure observations well, but some areas of possible disagreement between theory and observations still persist. The most serious small scale problem regards the origin and angular momentum in galaxies (Primack 2004). Two "angular momentum problems" prevent the formation of realistic spiral galaxies in numerical simulations (Primack 2004): i) overcooling in merging satellites with too much transfer of angular momentum to the dark halo and ii) the wrong distribution of specific angular momentum in halos, if the baryonic material has the same angular momentum distribution as dark matter halo. Detection of gravito-magnetic effects in gravitational lensing systems due to the spin of the deflector, either through time-delays measurements, as discussed in this paper, or through observations of the rotation of the plane of polarization of light waves from the background source (Sereno 2004), could provide direct estimates of angular momentum and help in developing a better understanding of astrophysics in galaxies.

REFERENCES

- Biggs A. D., Browne I. W. A., Helbig P., Koopmans L. V. E. et al., 1999, *MNRAS*, 304, 349
 Capozziello S., Cardone V. F., Re V., Sereno M., 2003, *MNRAS*, 343, 360
 Capozziello S., Re V., 2001, *Phys. Lett. A*, 290, 115
 Ciufolini I., Kopeikin S., Mashhoon B., Ricci F., 2003, *Phys. Lett. A*, 308, 101
 Ciufolini I., Pavlis E., 1998, *Science*, 279, 2100
 Ciufolini I., Pavlis E., 2004, *Nat.*, 431, 958
 Ciufolini I., Ricci F., 2002, *Class. Quantum Grav.*, 19, 3863
 Ciufolini I., Ricci F., 2003, gr-qc/0301030
 Ciufolini I., Wheeler J., 1995, *Gravitation and inertia*. (Princeton University Press, Princeton)
 Dymnikova I. G., 1986, in *IAU Symp. 114: Relativity in Celestial Mechanics and Astrometry*. High Precision Dynamical Theories and Observational Verifications Gravi-

- tational time delay of signals in the Kerr metric. pp 411-416
- Fomabnt E. B., Kopeikin S. M., 2003, *ApJ*, 598, 704
- Glicenstein J. F., 1999, *A & A*, 343, 1025
- Kochanek C. S., Schechter P. L., 2004, in *Measuring and Modeling the Universe: The Hubble Constant from Gravitational Lens Time Delays*. p. 117
- Kopeikin S., 1997, *J. Math. Phys.*, 38, 2587
- Kopeikin S., 2004, *Class. Quantum Grav.*, 21, 3251
- Kopeikin S., Mashhoon B., 2002, *Phys. Rev. D*, 65, 064025
- Kopeikin S. M., Schäfer G., 1999, *Phys. Rev. D*, 60, 124002
- Moh J., Mao S., White S. D. M., 1998, *MNRAS*, 295, 319
- Padmanabhan T., 2002, *Theoretical Astrophysics, Vol. III*. Cambridge University Press, Cambridge
- Peters A. O., Levine H., Wambsganss J., 2001, *Singularity theory and gravitational lensing*. Birkhauser, Boston
- Princk J. R., 2004, in *IAU Symposium: The Origin and Distribution of Angular Momentum in Galaxies*. p. 467
- Refsdal S., 1964, *MNRAS*, 128, 307
- Schneider P., Ehlers J., Falco E. E., 1992, *Gravitational Lenses*. (Springer-Verlag, Berlin)
- Sereno M., 2002, *Phys. Lett. A*, 305, 7
- Sereno M., 2003a, *MNRAS*, 344, 942
- Sereno M., 2003b, *Phys. Rev. D*, 67, 064007
- Sereno M., 2004, *MNRAS*, in press; astro-ph/0410015
- Sereno M., Cardone V. F., 2002, *A & A*, 396, 393
- Vitvitska M., Klypin A. A., Kuvshinov A. V., Wechsler R. H. et al., 2002, *ApJ*, 581, 799
- Weinberg S., 1972, *Gravitation and cosmology*. Wiley, New York